Journals Pub

International Journal of
Structural Engineering and Analysis

ISSN: 2456-5326
Volume 10, Issue 1, 2024
DOI (Journal): 10.37628/IJSEA

https://journalspub.com/journal/ijsea/

Research IJSEA

Comparative Structural Analysis of I-Girder and Box-Girder Designs in Flyover Bridges

Raju Ramrao Kulkarni[1,*], A.B. Vawhale[2]

Abstract

Bridge structures are vital for improving transportation in urban and suburban areas by offering routes that reduce traffic congestion. As urbanization accelerates in many metropolitan cities across India, the necessity for such infrastructure becomes increasingly important. This research aims to explore the structural behavior of flyover bridges, specifically focusing on 30-meter I-girder and 30-meter box-girder bridge segments under various loading conditions, in compliance with Indian Road Congress (IRC) standards. The bridge girders are modeled using plate elements in the STAAD Pro software. The study examines the structural performance of the girders by analyzing axial forces, shear forces, bending moments, and principal stresses under both dead and live loads. The design considerations include using reinforced cement concrete and prestressed concrete for the deck slab and girders, while piers and foundations are constructed with reinforced cement concrete. Prestressing techniques are utilized to enhance the structural performance, particularly to withstand maximum tensile stresses effectively.

Keywords: Box girder, traffic volume, IRC, prestressed concrete, FEM

INTRODUCTION

Background

Bridges serve as critical infrastructure, providing passage over obstacles such as rivers, valleys, or roads. Their designs vary significantly, tailored to meet the specific demands of different terrains and uses. Concrete is a fundamental material in bridge construction, utilized in components like foundations, abutments, piers, and decks. Its versatility allows for the creation of complex shapes and high span-to-depth ratios, making it an ideal choice for modern bridge designs [1–8].

Objective

This research aims to:

1. Conduct a comprehensive structural analysis and design of a flyover bridge according to Indian Road Congress (IRC) standards.
2. Investigate the behavior of key structural components, such as the deck slab and girders.
3. Compare the analysis and design of a 30-meter I Girder Bridge with a 30-meter prestressed concrete box girder.

***Author for Correspondence**
Raju Ramrao Kulkarni
E-mail: rajuanshu3@gmail.com

[1]Student, Department of Civil Engineering, Shreeyash College of engineering, Aurangabad, Maharashtra, India
[2]Assistant Professor, Civil Engineering Department, Shreeyash. College of engineering Aurangabad, Maharashtra, India

Received Date: June 01, 2024
Accepted Date: June 04, 2024
Published Date: June 06, 2024

Citation: Raju Ramrao Kulkarni, A.B. Vawhale. Comparative Structural Analysis of I-Girder and Box-Girder Designs in Flyover Bridges. International Journal of Structural Engineering and Analysis. 2024; 10(1): 1–14p.

What is a Flyover Bridge?

A flyover bridge, or overpass, is a structure that allows one roadway or railway line to pass over another. This design facilitates smoother communication between different transportation routes and helps reduce traffic congestion, especially in urban areas [9–15].

Necessity for the Construction of Flyover Bridges

Flyover bridges become essential in scenarios where expanding traditional roadways is not feasible, such as at busy railway crossings or in highly congested traffic areas. They provide a practical solution to alleviate traffic bottlenecks and enhance transportation efficiency [16–22].

Aesthetics

The aesthetic potential of concrete allows for a wide range of finishes and forms, ensuring that bridges can be designed to blend seamlessly with their surroundings and even enhance the visual appeal of the area. Given that bridges are often expected to last over a century, aesthetic considerations play a crucial role. Designs strive for slender, balanced decks and minimal bulk in end supports, while precast concrete elements can introduce unique visual effects and a sense of individuality.

Advantages of Flyover Construction

- Enhances traffic flow and control systems.
- Provides travelers with elevated, panoramic views.
- Maximizes road space by creating additional lanes overhead, reducing the need for extensive land acquisition.
- Reduces pollution and accident risks, resulting in time and fuel savings for commuters.
- Improves the aesthetic appeal of the cityscape, contributing to the overall urban design.

These factors collectively underscore the importance and benefits of flyover bridges in modern urban planning and infrastructure development (Figure 1).

Figure 1. Flyover bridge.

SYSTEM DEVELOPMENT AND METHODOLOGY

Our project focuses on the analysis and design of bridge components using the STAAD Pro software. This process includes manual load calculations and structural analysis, adhering to the minimum requirements outlined by the Indian Road Congress (IRC) to ensure structural safety.

Advantages of Using STAAD Pro

- *User-Friendly Interface:* Simplifies model generation and analysis.
- *Compliance with Indian Standards:* Ensures designs adhere to relevant codes.
- *Versatile Problem-Solving:* Capable of handling a wide range of structural problems.
- *Accurate Solutions:* Provides reliable and precise analysis results.

STAAD Pro offers a comprehensive suite of features, including visualization tools, advanced finite element analysis, and dynamic analysis capabilities. It is extensively used for designing various structures, such as buildings, bridges, culverts, and petrochemical plants.

STAAD Pro V8i

STAAD Pro allows for the individual design of structural members, performing operations, such as code checking, member selection, and optimization. Users can define members, load cases, and design parameters and iteratively perform design operations to meet specific requirements.

STAAD Pro User Interface

The graphical user interface (GUI) of STAAD Pro facilitates model creation, analysis, and visualization of results. The analysis and design engine supports integrated design for steel, concrete, timber, and aluminum structures.

Types of Structures

STAAD Pro can analyze and design structures comprising frame, plate/shell, and solid elements. For our project, we focus on space-type structures for bridge component design.

Supports

In STAAD Pro, supports can be defined as pinned, fixed, with partial releases. In our design, the supports are fixed, providing restraints against all directions of movement.

Grouping of Members

Girders are grouped based on loading conditions, such as bending moments and type of support. Longitudinal and cross-girders are categorized separately.

Generation of Member Property

Member properties are defined in STAAD Pro by selecting the member section and specifying dimensions according to loading conditions and their position in the structure.

Loadings on Structure

Loadings, including self-weight, dead load, live load, and seismic load, are manually specified and generated using STAAD Pro's load generator. Load cases are categorized and defined accordingly.

Analysis Facilities

STAAD Pro offers stiffness analysis, multiple analysis capabilities, and post-processing facilities. Deflection checks, code compliance, and analysis assumptions are integral parts of the design process.

Finite Element Method (FEM)

FEM is employed for the computer-based solution of complex structural problems. It involves dividing the structure into small elements, assembling stiffness matrices, and solving mathematical models to obtain accurate analysis results.

By leveraging STAAD Pro's capabilities and adhering to IRC standards, our project aims to ensure the structural safety and integrity of bridge components.

Research Data

Material Properties

Table 1 lists the material properties and geometric parameters considered for this study.

Table 1. Lists the material properties and geometric parameters.

S.N.	Design Parameter	Value
1	Unit weight of concrete	23.56 kN/m³
2	Unit weight of infill walls	20 kN/m³
3	Characteristic strength of concrete	20 N/mm²
4	Characteristic strength of steel	500 N/mm²

Structural Elements

Table 2 lists the dimensions of the structural elements considered for this study.

Table 2. Lists the dimensions of the structural elements.

S.N.	Design Parameter	Value
1	Girder for 20 meter span	600 mm x 1400 mm
2	Girder for 30 meter span	600 mm x 1800 mm
3	Cross girder	300 mm x 800 mm
4	Piers	3000/2500 mm
5	Slab thickness	380 mm
6	Kerbs thickness	230 mm

Loads Considered

The following types of loads were considered during the design process:

1. Self-weight of the girders.
2. Weight of the slab.
3. Live load of 4 kN/m².
4. Floor finish weight of 1 kN/m².

Descriptions of Drafted Models

1. *Model 1:* A 30-meter-span I-girder double lane bridge analyzed for dead load and live load as per IRC standards.
2. *Model 2:* A 30-meter span-box girder double lane bridge analyzed for dead load and live load as per IRC standards.
3. *Model 3:* A 30-meter-span I-girder model for piers.
4. *Model 4:* A 30-meter-span box girder model for piers.

By following this methodology and using STAAD Pro for analysis and design, the project ensures that the bridge components meet all necessary safety and performance standards. Tables 3–15 and Figures 2–13.

Table 3. Analysis Tables of a 30-meter R.C.C span girder beam end force summary for dead load (OGEND).

	Beam	L/C	Axial	Shear		Torsion	Bending	
			Fx (kN)	*Fy (kN)*	*Fz (kN)*	*Mx (kNm)*	*My (kNm)*	*Mz (kNm)*
Max Fx	1290	1: DEADLOAD	**33.643**	0.000	0.000	0.000	0.000	0.000
Min Fx	11	1: DEADLOAD	**0.000**	0.571	0.000	0.030	0.000	0.099
Max Fy	26	1: DEADLOAD	0.000	**909.344**	0.000	0.000	0.000	0.000
Min Fy	1321	1: DEADLOAD	0.000	**-909.343**	0.000	0.000	0.000	-0.000
Max Fz	11	1: DEADLOAD	0.000	0.571	**0.000**	0.030	0.000	0.099
Min Fz	11	1: DEADLOAD	0.000	0.571	**0.000**	0.030	0.000	0.099

Max Mx	38	1: DEADLOAD	0.000	1.510	0.000	**0.037**	0.000	0.225
Min Mx	46	1: DEADLOAD	0.000	1.510	0.000	**-0.037**	0.000	0.225
Max My	11	1: DEADLOAD	0.000	0.571	0.000	0.030	**0.000**	0.099
Min My	11	1: DEADLOAD	0.000	0.571	0.000	0.030	**0.000**	0.099
Max Mz	38	1: DEADLOAD	0.000	1.510	0.000	0.037	0.000	**0.225**
Min Mz	48	1: DEADLOAD	0.000	821.702	0.000	0.000	0.000	**-1.73E 3**

Table 4. Beam end force summary for moving load (OGEND).

	Beam	**L/C**	**Axial**	**Shear**		**Torsion**	**Bending**	
			Fx (kN)	***Fy (kN)***	***Fz (kN)***	***Mx (kNm)***	***My (kNm)***	***Mz (kNm)***
Max Fx	1290	87: LOAD GEN	**133.873**	0.000	0.000	0.000	0.000	0.000
Min Fx	1290	463: LOAD GEN	**-11.027**	0.000	0.000	0.000	0.000	0.000
Max Fy	30	460: LOAD GEN	0.000	**490.433**	0.000	0.000	0.000	0.000
Min Fy	1321	468: LOAD GEN	0.000	**-466.222**	0.000	0.000	0.000	-466.2
Max Fz	11	2: LOAD GEN	0.000	35.411	**0.000**	-0.001	0.000	6.613
Min Fz	11	2: LOAD GEN	0.000	35.411	**0.000**	-0.001	0.000	6.613
Max Mx	46	553: LOAD GEN	0.000	0.052	0.000	**0.058**	0.000	0.018
Min Mx	38	539: LOAD GEN	0.000	0.052	0.000	**-0.058**	0.000	0.018
Max My	11	2: LOAD GEN	0.000	35.411	0.000	-0.001	**0.000**	6.613
Min My	11	2: LOAD GEN	0.000	35.411	0.000	-0.001	**0.000**	6.613
Max Mz	1311	485: LOAD GEN	0.000	57.890	0.000	0.010	0.000	**12.29**
Min Mz	48	433: LOAD GEN	0.000	455.097	0.000	0.000	0.000	**-922.99**

Table 5. Analysis of a R.C.C 30-meter span girder.

SPAN	**FORCE**	**DL**	**LL**	**TOTAL**
OGEND	Shear	1040	506	**1546**
	Moment	1960	941	2901
OGMID	Shear	60	230	290
	Moment	7780	3120	**10900**
OGQSPAN	Shear	651	358	1009
	Moment	5590	2360	7950
MGEND	Shear	949	443	1392
	Moment	1800	805	2605
MGMID	Shear	58	177	235
	Moment	7440	2690	10130
MGQSPAN	Shear	641	329	970
	Moment	5280	2010	7290
SGR	Shear	54	106	160
	Moment	109	225	334

Table 6. Analysis of a 30-meter-span box girder (dead load).

SPAN	FORCE	GIRDER	SLAB	SIDL	LIVE	TOTAL
OGEND	Shear	334	411	295	506	**1546**
	Moment	619	786	555	941	2901
OGMID	Shear	24	18	18	230	290
	Moment	2490	3100	2190	3120	**10900**
OGQSPAN	Shear	221	255	175	358	1009
	Moment	1780	2230	1580	2360	7950
MGEND	Shear	330	380	239	443	1392
	Moment	612	730	458	805	2605
MGMID	Shear	23	17	18	177	235
	Moment	2460	2990	1990	2690	10130
MGQSPAN	Shear	221	253	167	329	970
	Moment	1760	2130	1390	2010	7290
SGR	Shear	8	22	24	106	160
	Moment	15	47	47	225	334

Table 7. Dead load stresses summary for bottom end.

	Plate	L/C	Principal		Von Mis		Tresca	
			Top ***(N/mm²)***	***Bottom*** ***(N/mm²)***	***Top*** ***(N/mm²)***	***Bottom*** ***(N/mm²)***	***Top*** ***(N/mm²)***	***Bottom*** ***(N/mm²)***
Max (t)	56880	1: DEADLOAD	**10.062**	4.671	16.611	14.055	19.173	15.795
Max (b)	71564	1: DEADLOAD	-5.027	**16.336**	15.203	14.554	17.080	16.336
Max VM (t)	74573	1: DEADLOAD	6.389	6.732	**17.589**	11.426	19.890	13.193
Max VM (b)	48335	1: DEADLOAD	-4.852	16.434	15.193	**14.631**	17.026	16.434
Tresca (t)	74573	1: DEADLOAD	6.389	6.732	17.589	11.426	**19.890**	13.193
Tresca (b)	48335	1: DEADLOAD	-4.852	16.434	15.193	14.631	17.026	**16.434**

Table 8. Dead load stresses summary for top end.

	Plate	L/C	Principal		Von Mis		Tresca	
			Top ***(N/mm²)***	***Bottom*** ***(N/mm²)***	***Top*** ***(N/mm²)***	***Bottom*** ***(N/mm²)***	***Top*** ***(N/mm²)***	***Bottom*** ***(N/mm²)***
Max (t)	56615	1: DEADLOAD	**4.893**	-1.023	4.798	3.622	4.893	4.024
Max (b)	48689	1: DEADLOAD	-0.939	**5.598**	3.944	5.261	4.328	5.598
Max VM (t)	56183	1: DEADLOAD	4.620	-1.303	**5.086**	3.440	5.451	3.901
Max VM (b)	56897	1: DEADLOAD	-0.346	6.814	3.534	**6.544**	3.694	6.814
Tresca (t)	74270	1: DEADLOAD	4.437	-1.417	5.029	3.361	**5.462**	3.837
Tresca (b)	56897	1: DEADLOAD	-0.346	6.814	3.534	6.544	3.694	**6.814**

Analysis Summery of 30-meter Span Box girder (Live Load)

Analysis A 30-meter-span box girder (live load) is described in Tables 11–15.

Table 9. Dead load stresses summary for bottom mid.

	Plate	L/C	Principal		Von Mis		Tresca	
			Top (N/mm^2)	*Bottom* (N/mm^2)	*Top* (N/mm^2)	*Bottom* (N/mm^2)	*Top* (N/mm^2)	*Bottom* (N/mm^2)
Max (t)	52739	1: DEADLOAD	**3.952**	2.925	4.078	2.736	4.194	2.925
Max (b)	73750	1: DEADLOAD	3.265	**2.484**	3.453	2.285	3.614	2.484
Max VM (t)	52739	1: DEADLOAD	3.952	2.925	**4.078**	2.736	4.194	2.925
Max VM (b)	73091	1: DEADLOAD	3.939	2.744	3.800	**2.752**	3.939	2.760
Tresca (t)	52739	1: DEADLOAD	3.952	2.925	4.078	2.736	**4.194**	2.925
Tresca (b)	52739	1: DEADLOAD	3.952	2.925	4.078	2.736	4.194	**2.925**

Table 10. Dead load stresses summary for top mid.

	Plate	L/C	Principal		Von Mis		Tresca	
			Top (N/mm^2)	*Bottom* (N/mm^2)	*Top* (N/mm^2)	*Bottom* (N/mm^2)	*Top* (N/mm^2)	*Bottom* (N/mm^2)
Max (t)	56615	1: DEADLOAD	**4.893**	-1.023	4.798	3.622	4.893	4.024
Max (b)	48689	1: DEADLOAD	-0.939	**5.598**	3.944	5.261	4.328	5.598
Max VM (t)	56183	1: DEADLOAD	4.620	-1.303	**5.086**	3.440	5.451	3.901
Max VM (b)	56897	1: DEADLOAD	-0.346	6.814	3.534	**6.544**	3.694	6.814
Tresca (t)	74270	1: DEADLOAD	4.437	-1.417	5.029	3.361	**5.462**	3.837
Tresca (b)	56897	1: DEADLOAD	-0.346	6.814	3.534	6.544	3.694	**6.814**

Table 11. Live load stresses summary for bottom end.

	Plate	L/C	Principal		Von Mis		Tresca	
			Top (N/mm^2)	*Bottom* (N/mm^2)	*Top* (N/mm^2)	*Bottom* (N/mm^2)	*Top* (N/mm^2)	*Bottom* (N/mm^2)
Max (t)	56880	70: LOAD	**3.399**	2.316	6.254	5.075	7.217	5.820
Max (b)	48363	129: LOAD	-1.649	**4.756**	6.758	4.154	7.430	4.756
Max VM (t)	48363	129: LOAD	-1.649	4.756	**6.758**	4.154	7.430	4.756
Max VM (b)	56880	70: LOAD	3.399	2.316	6.254	**5.075**	7.217	5.820
Tresca (t)	56881	70: LOAD	2.283	3.271	6.622	4.895	**7.461**	5.628
Tresca (b)	56880	70: LOAD	3.399	2.316	6.254	5.075	7.217	**5.820**

Table 12. Live load stresses summary for top end.

	Plate	L/C	Principal		Von Mis		Tresca	
			Top (N/mm^2)	*Bottom* (N/mm^2)	*Top* (N/mm^2)	*Bottom* (N/mm^2)	*Top* (N/mm^2)	*Bottom* (N/mm^2)
Max (t)	48338	29: LOAD	**5.620**	-0.595	5.307	4.969	5.620	5.239
Max (b)	48976	29: LOAD	-0.551	**4.046**	3.533	3.792	3.777	4.046
Max VM (t)	48338	29: LOAD	5.620	-0.595	**5.307**	4.969	5.620	5.239
Max VM (b)	48338	29: LOAD	5.620	-0.595	5.307	**4.969**	5.620	5.239
Tresca (t)	48338	29: LOAD	5.620	-0.595	5.307	4.969	**5.620**	5.239
Tresca (b)	48338	29: LOAD	5.620	-0.595	5.307	4.969	5.620	**5.239**

Table 13. Live load stresses summary for bottom mid.

	Plate	L/C	Principal		Von Mis		Tresca	
			Top ***(N/mm²)***	***Bottom*** ***(N/mm²)***	***Top*** ***(N/mm²)***	***Bottom*** ***(N/mm²)***	***Top*** ***(N/mm²)***	***Bottom*** ***(N/mm²)***
Max (t)	56880	70: LOAD	**3.399**	2.316	6.254	5.075	7.217	5.820
Max (b)	48363	129: LOAD	-1.649	**4.756**	6.758	4.154	7.430	4.756
Max VM (t)	48363	129: LOAD	-1.649	4.756	**6.758**	4.154	7.430	4.756
Max VM (b)	56880	70: LOAD	3.399	2.316	6.254	**5.075**	7.217	5.820
Tresca (t)	56881	70: LOAD	2.283	3.271	6.622	4.895	**7.461**	5.628
Tresca (b)	56880	70: LOAD	3.399	2.316	6.254	5.075	7.217	**5.820**

Table 14. Dead load stresses summary for top mid.

	Plate	L/C	Principal		Von Mis		Tresca	
			Top ***(N/mm²)***	***Bottom*** ***(N/mm²)***	***Top*** ***(N/mm²)***	***Bottom*** ***(N/mm²)***	***Top*** ***(N/mm²)***	***Bottom*** ***(N/mm²)***
Max (t)	50698	35: LOAD	**2.217**	-0.934	2.486	1.851	2.687	2.132
Max (b)	72387	155: LOAD	-1.082	**1.800**	1.721	1.741	1.984	1.800
Max VM (t)	72396	57: LOAD	2.188	-0.851	**2.495**	1.826	2.717	2.096
Max VM (b)	72391	56: LOAD	-0.889	1.751	1.564	**1.854**	1.806	1.942
Tresca (t)	72396	57: LOAD	2.188	-0.851	2.495	1.826	**2.717**	2.096
Tresca (b)	50698	35: LOAD	2.217	-0.934	2.486	1.851	2.687	**2.132**

Table 15. Summary of shear force and bending moment for 30-meter I girder and 30-meter span girders.

S.N.	**Particulars**	**Dead load**	**Live load**	**Total**
30-meter I girder bridge				
1	Axial force (kN)	4380	1180	***5560***
2	Design moment (kN)	4670	1860	***6530***
30-meter box girder bridge				
1	Axial force (kN)	4930	839	***5769***
2	Design moment (kN)	10000	2220	***12220***

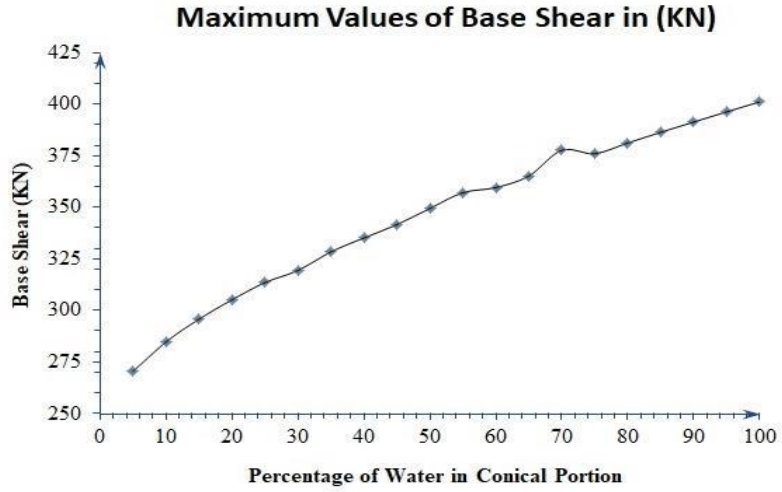

Figure 2. Values of base shear for empty tank conditions.

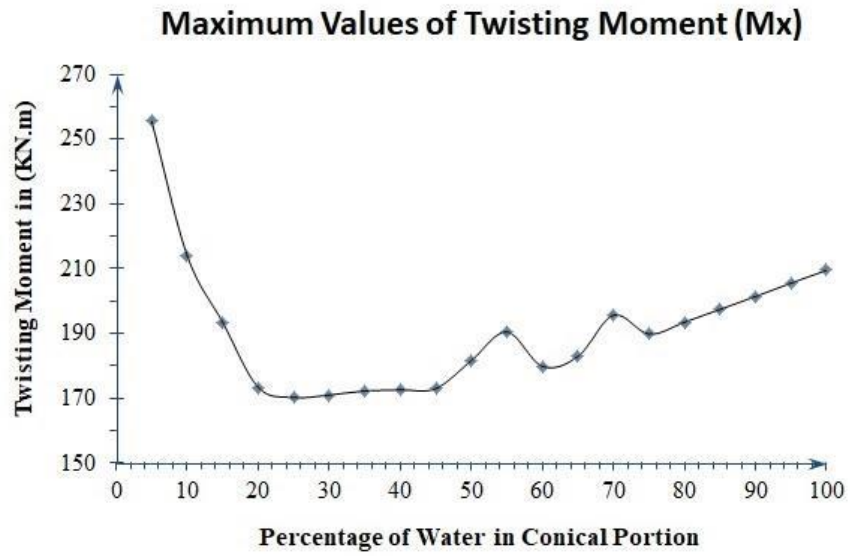

Figure 3. Values of moment in x-direction for empty tank conditions.

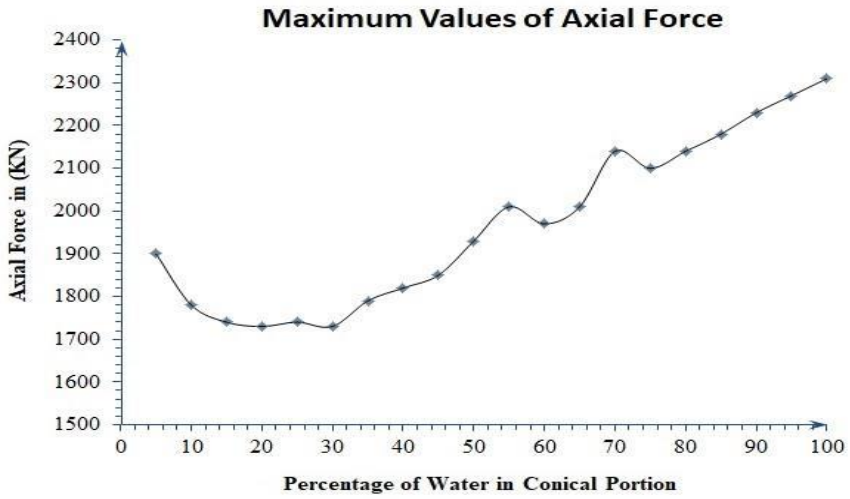

Figure 4. Value of axial force for empty tank conditions.

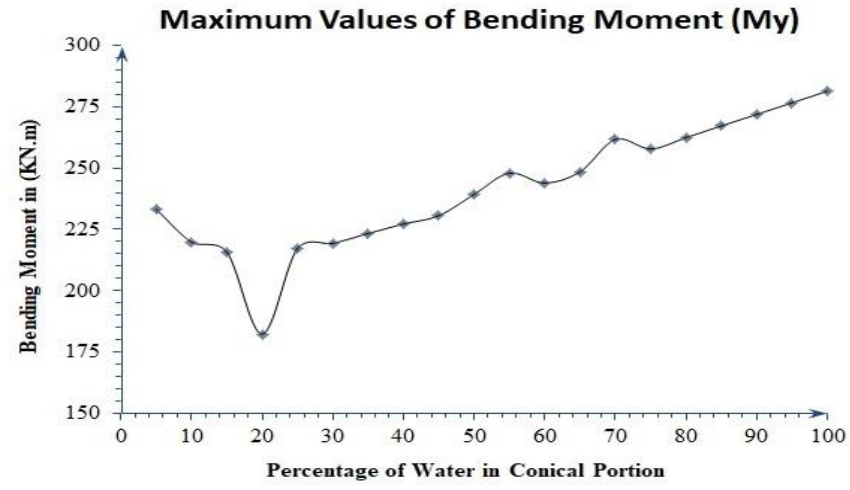

Figure 5. Values of the moment in the y-direction for empty tank conditions.

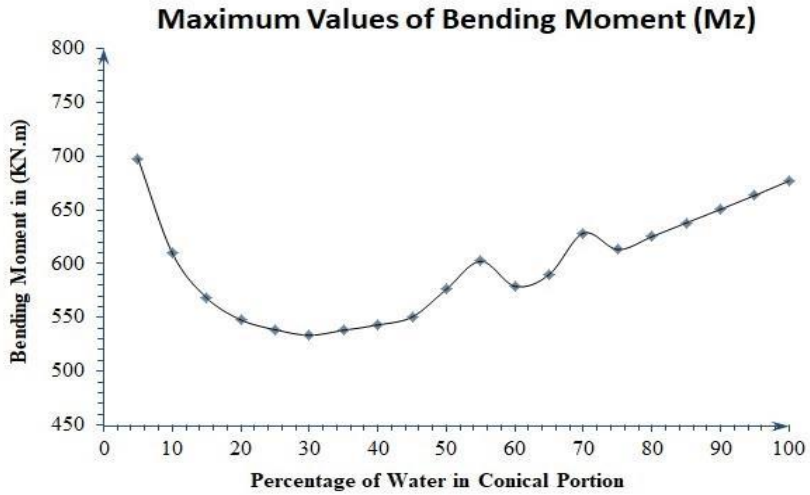

Figure 6. Values of the moment in the z-direction for empty tank conditions.

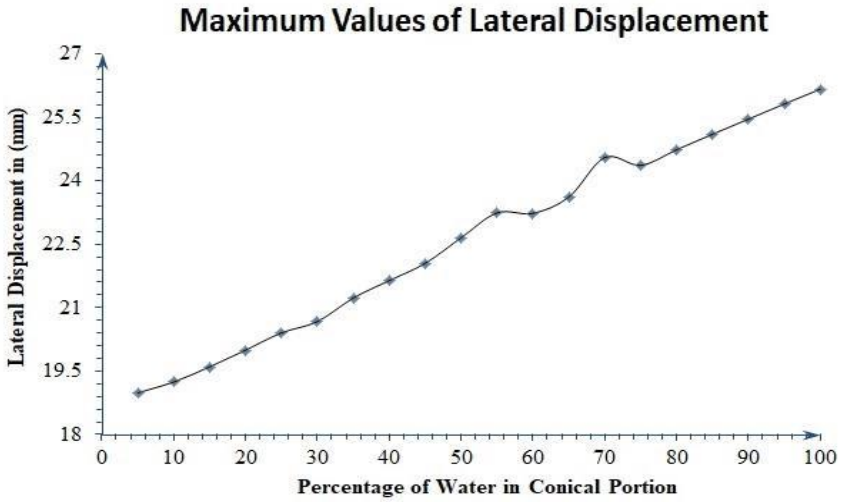

Figure 7. Values of lateral displacement for the empty tank conditions.

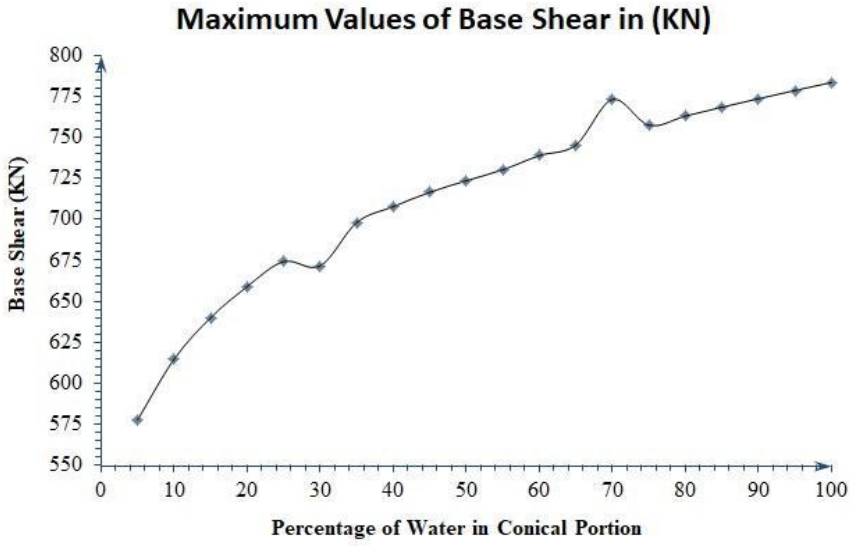

Figure 8. Values of base shear for full tank conditions.

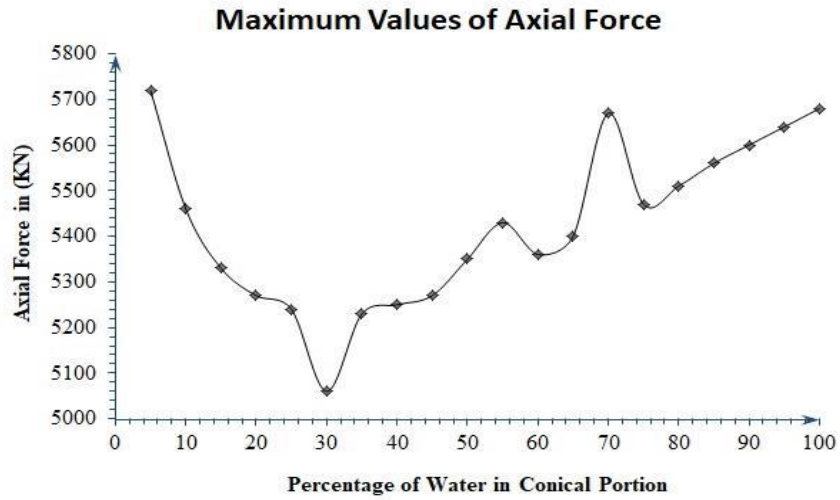

Figure 9. Value of axial force for full tank condition.

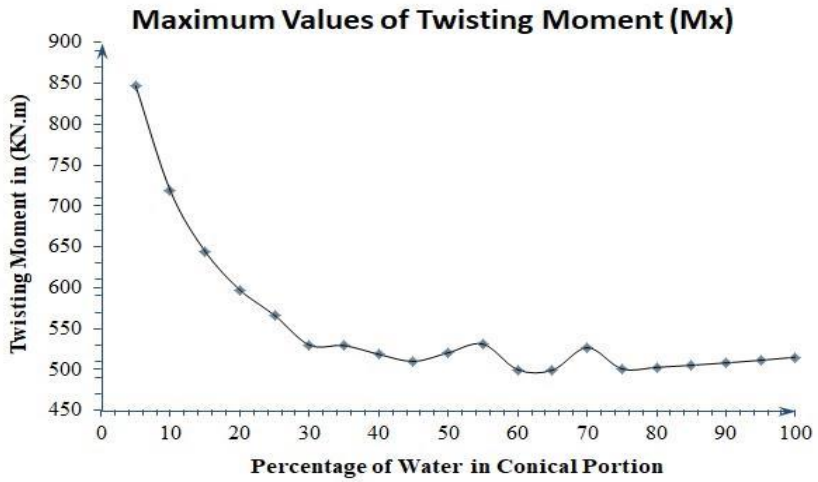

Figure 10. Values of moment in x-direction for full tank conditions.

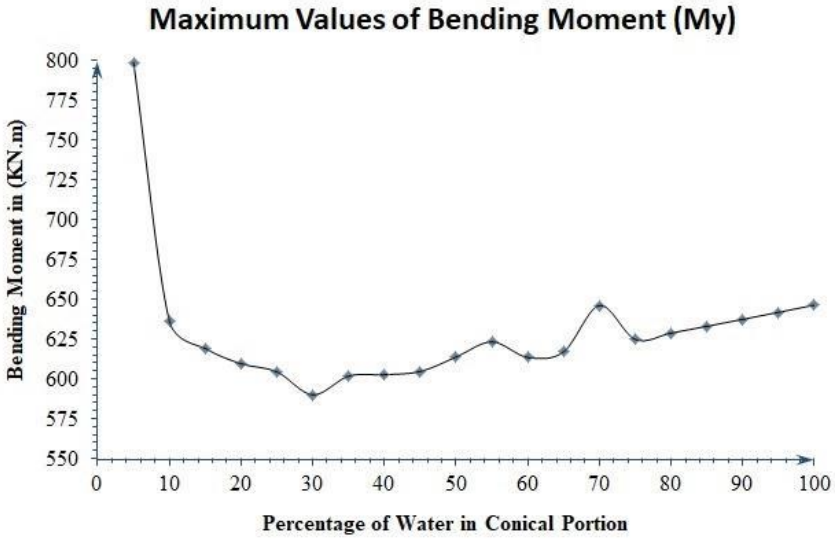

Figure 11. Values of moment in y-direction for full tank conditions.

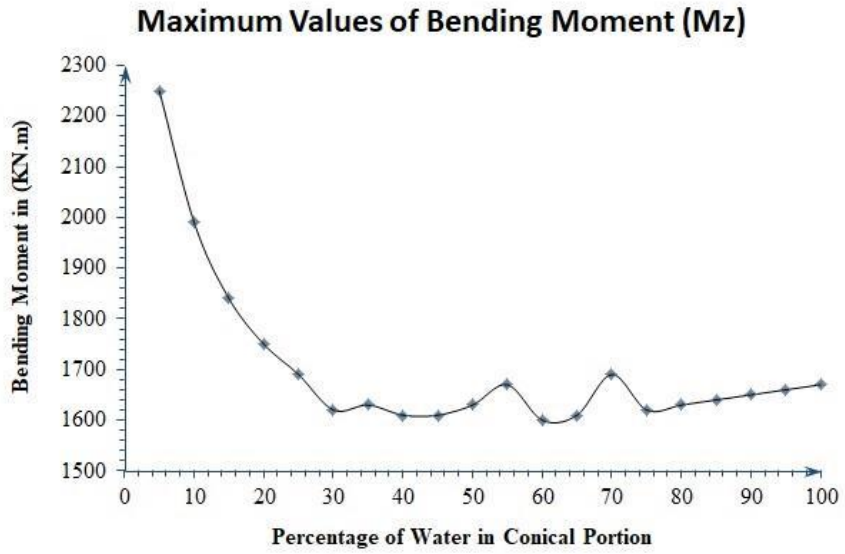

Figure 12. Values of moment in z-direction for full tank conditions.

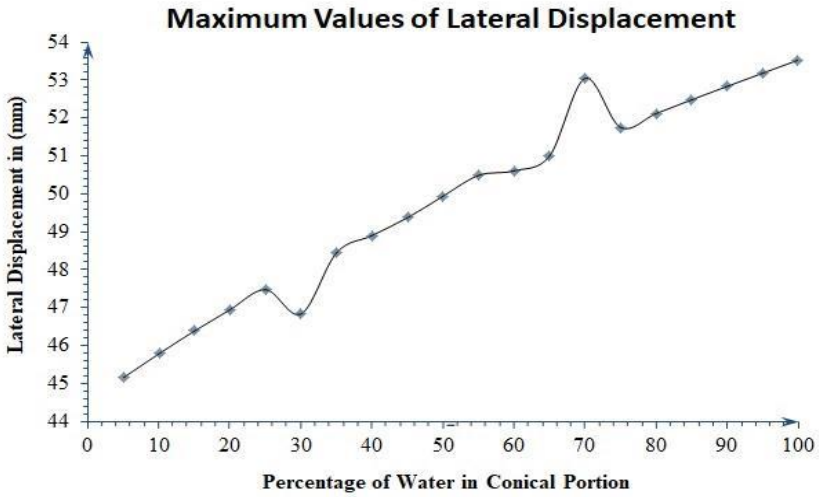

Figure 13. Values of lateral displacement for full tank conditions.

DISCUSSION THROUGH GRAPHS

Base Shear

- The graphs demonstrate a direct correlation between the water percentage in the conical part and the resulting base shear for both empty and full tank conditions.
- The maximum base shear is observed when the conical part is fully filled (pure conical tank), while the minimum base shear occurs when the conical part is empty for both conditions.

Axial Force

- The highest axial force is recorded when the conical part is at full capacity in both empty and full tank scenarios.
- The lowest axial force is noted when the conical part contains 30% water in both empty and full tank conditions.

Bending Moment (Mx and Mz)

- The graphs reveal that the highest twisting moment (Mx) and bending moment (Mz) occur in a pure cylindrical tank (with no water in the conical tank).

- For empty tank conditions, the minimum twisting and bending moments are observed with 30% water in the conical part. For full tank conditions, the minimum moments occur with 60% water in the conical part.

Bending Moment (My)

- The maximum bending moment (My) is recorded when the conical part is fully filled for empty tank conditions.
- For full tank conditions, the maximum bending moment (My) is seen when the conical part is empty (pure cylindrical tank), while the minimum occurs with 30% water in the conical part.

Lateral Displacement

- The graphs indicate that an increase in the water percentage in the conical part leads to greater lateral displacement for both empty and full tank conditions.
- The optimal displacement is achieved when the conical part contains 30% water for both scenarios.
- Importantly, all recorded lateral displacement values are within the limits specified by IS-1893-2002, which sets the maximum roof displacement limit at 0.004 times the height of the structure.

CONCLUSION

It is concluded that:

The highest base shear occurs when the conical tank is completely filled with water (pure conical tank), whereas the lowest base shear is observed when the conical section contains no water (cylindrical tank), under both empty and full tank conditions.

Optimal results for forces acting in the Y-direction (base shear, axial force, bending moment (My) and displacements are achieved with the conical part containing 30% water for both empty and full tank conditions, maintaining a ratio of conical

= 30:70.

For forces acting in the X and Z directions (twisting moment (Mx), bending moment (Mz), the best outcomes are achieved with the conical part containing 60% water for both empty and full tank conditions, maintaining a ratio of conical

= 60:40.

The lateral displacement values remain within the specified limits as per IS-1893-2002.

REFERENCES

1. Housner GW. The dynamic behavior of water tanks. Bull Seismol Soc Am. 1963;53(2):381–387. doi:10.1785/BSSA0530020381.
2. El Damatty AA, Korol RM, Mirza FA. Stability of imperfect steel conical tanks under hydrostatic loading. J Struct Eng. 1997;123(6):703–712. doi:10.1061/(ASCE)0733-9445(1997)123:6(703).
3. El Damatty AA, EI-Attar MB, Korol RM. Inelastic stability of conical tanks. J Thin-Walled Struct. 1998;31(4):343–359. doi:10.1016/S0263-8231(98)00020-2.
4. El Damatty AA, Marroquin EG, Attar ME. Behavior of stiffened liquid-filled conical tanks. J Thin-Walled Struct. 2001;39(4):353–373. doi:10.1016/S0263-8231(01)00005-2.
5. El Damatty AA, Marroquin E. Design procedure for stiffened water-filled steel conical tanks. J Thin-Walled Struct. 2002;40(3):263–282. doi:10.1016/S0263-8231(01)00052-0.
6. Sweedan AMI, El Damatty AA. Experimental and analytical evaluation of the dynamic characteristics of conical shells. J Thin-Walled Struct. 2002;40(5):465–486. doi:10.1016/S0263-8231(01)00070-2.
7. Sweedan AMI, EI Damatty AA. Equivalent models of pure conical tanks under vertical ground excitation. J Struct Eng. 2005;131(5):725–733. doi:10.1061/(ASCE)0733-9445(2005)131:5(725).

8. EI Damatty AA, Saafana MS, Sweedan AMI. Dynamic characteristics of combined conical-cylindrical shells. J Thin-Walled Struct. 2005;43(9):1380–1397. doi:10.1016/j.tws.2005.04.002.
9. EI Damatty AA, Saafana MS, Sweedan AMI. Experimental study conducted on a liquid-filled combined conical tank model. J Thin-Walled Struct. 2005;43(9):1398–1417. doi:10.1016/j.tws. 2005.04.003.
10. EI Damatty AA, Sweedan AMI. Equivalent mechanical analog for dynamic analysis of pure conical tanks. J Thin-Walled Struct. 2006;44(4):429–440. doi:10.1016/j.tws.2006.03.016.
11. Sweedan AMI, EI Damatty AA. Simplified procedure for design of liquid-storage combined conical tanks. J Thin-Walled Struct. 2009;47(6–7):750–759. doi:10.1016/j.tws.2008.12.005.
12. Hafeez G, EI Ansary AM, EI Damatty AA. Stability of combined imperfect conical tanks under hydrostatic loading. J Constr Steel Res. 2010;66(11):1387–1397. doi:10.1016/j.jcsr.2010.05.007.
13. Hafeez G, EI Ansary AM, EI Damatty AA. Effect of wind loads on the stability of conical tanks. Canadian J Civil Eng. 2011;38(4):444–454. doi:10.1139/l11-017.
14. EI Ansary AA, EI Damatty AA. Behavior of elevated liquid-filled concrete conical tanks. General Conference at CSCE. Montréal, Québec. 2013, May 29 to June 1. CSCE. 1–10.
15. Jolie M, Hassan MM, EI Damatty AA. Assessment of current design procedures for conical tanks under seismic loading. J Civil Eng. 2013;40(12):1151–1163. doi:10.1139/cjce-2012-0318.
16. Jolie M, EI Ansary AM, EI Damatty AA. Seismic analysis of elevated pure conical tanks under vertical excitation. J Civil Eng. 2014;41(10):909–917. doi:10.1139/cjce-2014-0104.
17. Azabi TM, EI Damatty AA. Behaviour of reinforced concrete conical tanks under hydrostatic loading [Master's thesis]. London, (Canada): The University of Western Ontario, Civil and Environmental Engineering; 2014.
18. EIansary AA, EI Damatty AA, EI Ansary AM. Nonlinear behaviour of reinforced concrete conical tanks under hydrostatic pressure. J Civil Eng. 2016;43(2):85–98. doi:10.1139/cjce-2015-0198.
19. EI Ansary AA, EI Damatty AA, EI Ansary AM. Assessment of equivalent cylinder method and development of charts for analysis of concrete conical tanks. Eng Struct. 2016;126:27–39. doi:10.1016/j.engstruct.2016.06.053.
20. Musa A, EI Damatty AA. Capacity of liquid-filled steel conical tanks under vertical excitation. J Thin-Walled Struct. 2016;103:199–210. doi:10.1016/j.tws.2016.02.012.
21. EI Ansary AA, EI Damatty AA. Behaviour of composite conical tanks under hydrostatic pressure. Eng Struct. 2017;134:172–189. doi:10.1016/j.engstruct.2016.12.041.
22. Criteria for earthquake resistant design of structures (Part-II, liquid retaining tanks) (IS: 1893-2002). New Delhi: Bureau of Indian Standards.

